

Structure and electronic properties of Mg-doped β -rhombohedral boron constructed from icosahedral clusters

H. Hyodo,^{1,*} S. Araake,^{1,†} S. Hosoi,¹ K. Soga,² Y. Sato,³ M. Terauchi,³ and K. Kimura¹

¹*Department of Advanced Materials Science, The University of Tokyo, 277-8561 Chiba, Japan*

²*Department of Materials Science and Technology, Tokyo University of Science, 278-8510 Chiba, Japan*

³*Institute for Multidisciplinary Research for Advanced Materials, Tohoku University, 980-8577 Miyagi, Japan*

(Received 17 July 2006; revised manuscript received 10 August 2007; published 15 January 2008)

High- T_C superconductivity is possible upon metallic-element doping into β -rhombohedral boron (β -B₁₀₅), which is one of the boron icosahedral cluster solids. We attempted magnesium (Mg) doping into β -B₁₀₅ and discussed the possibility of metal transition and superconductivity. We achieved Mg doping into β -B₁₀₅ at a high Mg concentration of up to MgB_{11.5} (8.6 Mg/cell), i.e., electron doping sufficient for the Fermi energy (E_F) to reach the conduction band over the intrinsic acceptor level (IAL) and trapping levels. However, neither metal transition nor superconductivity was observed. The changes in the structure and electronic properties are discussed on the basis of the results of x-ray powder diffraction using the Rietveld method and electrical conductivity and magnetic susceptibility measurements, respectively. We estimated the density of states near E_F and discussed the electronic states of β -B₁₀₅. From the result, it is suggested that a localized state exists above the IAL probably originating from the B₂₈ cluster with structural defects.

DOI: 10.1103/PhysRevB.77.024515

PACS number(s): 74.10.+v, 61.66.Bi, 71.20.Ps, 81.05.Je

I. INTRODUCTION

Boron (B)-rich solids have a framework crystal structure built up from B₁₂ icosahedral clusters. These solids are called boron-icosahedral cluster solids (B-ICSs). B-ICSs have relatively large interstitial doping sites; thus, they can accept a large amount of other elements without destroying their original icosahedral cluster structures.¹⁻³ The high symmetry of the B₁₂ cluster, i.e., icosahedral symmetry, gives rise to the high degeneracy of the electronic states of this cluster, which accordingly results in the high density of states (DOS). If we can dope metallic elements into B-ICSs and donate electrons in a similar manner to alkali metals doping into C₆₀,^{4,5} and then adjust the Fermi energy (E_F) to a position of high DOS, high- T_C superconductivity can be expected.⁶ Table I shows a comparison between the layered solids and the cluster solids based on B and carbon (C). In the case of C-rich solids, K₃C₆₀, a cluster solid consisting of C₆₀ clusters that have the same icosahedral symmetry as B₁₂ clusters, has a much higher T_C (Ref. 4) than KC₈,⁷ a layered solid. There are two reasons for this. One is that K₃C₆₀ has a higher DOS at E_F [$N(E_F)$] (Ref. 8) than KC₈ (Ref. 9) owing to the high symmetry of C₆₀ clusters. The other is that high-frequency intra-cluster phonons couple strongly with conduction electrons for K₃C₆₀,⁵ whereas low-frequency bending modes do for KC₈,¹⁰ because E_F is located in the π band. On the other hand, in the case of B-rich solids, MgB₂ has a much higher T_C (Ref. 11) than the similarly layered KC₈, because E_F is located in the σ band, and higher-frequency stretching modes couple.¹² Furthermore, one can expect higher T_C , due to higher $N(E_F)$, for metal-doped B-ICSs than for layered MgB₂ (Ref. 13) as in the case of C-rich solids. According to first-principles calculations, lithium (Li)-doped α -rhombohedral B (see Table I) is predicted to have higher $N(E_F)$ than K₃C₆₀ and MgB₂ and to show superconductivity.⁶ Moreover, it is thought that B-ICSs have not only high $N(E_F)$ values but also high phonon frequencies¹⁴ and a large

electron-phonon coupling constant^{15,16} comparable to those of MgB₂. B-ICSs have favorable features for achieving high- T_C superconductivity.

B forms four allotropes: α - and β -rhombohedral B (α -B₁₂ and β -B₁₀₅) and α - and β -tetragonal B, all of which consist of B₁₂ clusters. Figure 1 shows the structures of α -B₁₂ and β -B₁₀₅ with major doping sites; β -B₁₀₅ is the subject of this research. For α -B₁₂, a B₁₂ cluster is located on each vertex of the rhombohedral unit cell. For β -B₁₀₅, four B₁₂ clusters are located on the corners and edge centers of the rhombohedral unit cell, a single B atom is located at the center of the unit cell, and two B₂₈ clusters, which are modified trios consisting of B₁₂ clusters, are arranged symmetrically to this atom, along the main body diagonal. The ideal structural formula of β -B₁₀₅ is given as (B₁₂)₄(B₂₈)₂B; however, it has partially occupied sites, i.e., the occupancy of B(B13) is approximately 75% and those of B(B16) to B(B20) are approximately 3%–25%. Therefore, the actual structural formula of

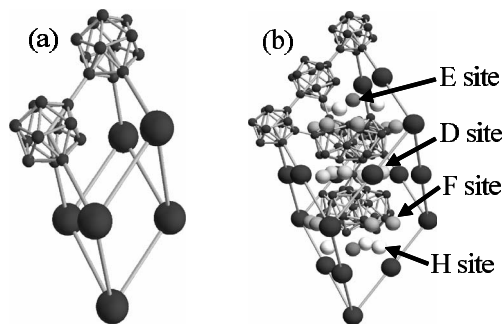
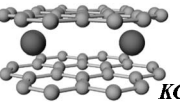
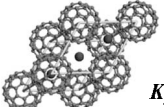
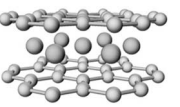
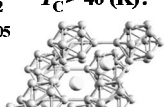


FIG. 1. Structures of (a) α -B₁₂ and (b) β -B₁₀₅ with major doping sites. α -B₁₂ has only a B₁₂ cluster; on the other hand, β -B₁₀₅ has not only B₁₂ clusters but also B₂₈ clusters as building blocks. β -B₁₀₅ is only the ideal structural formula and differs from the actual composition B_{106.6}; it has partially occupied sites, some of which are not shown in the figure.

TABLE I. Superconductivities of layered and cluster solids based on boron and carbon. The $N(E_F)$ values were calculated by referring to Refs. 9, 8, 13, and 6 for KC_8 , K_3C_{60} , MgB_2 , and LiB_{12} , respectively.

	Layered solids	Cluster solids
Carbon	KC_8 : $T_C \sim 0.1$ (K) $N(E_F) \sim 14$ (states/eV nm ³) $\omega \sim 170$ (cm ⁻¹) (Ref. 10)  KC_8	K_3C_{60} : $T_C \sim 20$ (K) $N(E_F) \sim 25$ (states/eV nm ³) $\omega \sim 500 - 1400$ (cm ⁻¹) (Ref. 5)  K_3C_{60}
Boron	MgB_2 : $T_C \sim 40$ (K) $N(E_F) \sim 24$ (states/eV nm ³) $\omega \sim 600$ (cm ⁻¹) (Ref. 12)  MgB_2	Li_3B_{12} : $N(E_F) \sim 39$ (states/eV nm ³) $\omega \sim 500 - 1200$ (cm ⁻¹) (Ref. 14) $Mg_{x}B_{12}$ $T_C > 40$ (K)? Mg_xB_{105}  Li_3B_{12}

β - B_{105} becomes $B_{106,6}$,¹⁷ however, we call β -rhombohedral boron β - B_{105} for convenience. The lattice constant of β - B_{105} is almost two times larger than that of α - B_{12} . Since the structure of α - B_{12} is simpler, first-principles calculations are mainly performed for α - B_{12} ; however, α - B_{12} cannot be easily prepared experimentally.¹⁸ Fusion certainly leads to the crystallization to β - B_{105} . α - B_{12} can only be prepared at temperatures below approximately 1470 K, which is approximately 1000 K lower than the melting point of B. Above this temperature, an irreversible transformation from α - B_{12} to β - B_{105} takes place. Therefore, β - B_{105} is more often used in experimental research.

We have reported studies on the doping of several metallic elements into β - B_{105} .^{19–22} Metal doping experiments are effective not only for attaining superconductivity but also for studying the electronic structure of β - B_{105} . β - B_{105} has gap states called the intrinsic acceptor level (IAL), or S2, and six intrinsic electron trapping levels, as determined from several experimental results.^{23–25} The origin of the IAL is considered to be the electron deficiency of B_{12} , the Jahn-Teller effect,^{26,27} and structural defects.^{28–30} From the results of Li doping into β - B_{105} , Li doping at most eight Li per cell only causes the filling of the IAL which can accept at most eight electrons per cell.¹⁹ Hence, it is necessary to dope more electrons to adjust E_F in the conduction band and to achieve metal transition and superconductivity. This adjustment may be possible by doping with more than eight electrons per cell, because the density of six electron trapping levels should be much smaller than that of the IAL.²³ We attempted the doping of magnesium (Mg) into β - B_{105} expecting the donation of two electrons. However, silicon (Si) impurity, considered to originate from the quartz tube used during Mg doping, was simultaneously doped into β - B_{105} and prevented Mg doping at a large amount exceeding four Mg per cell, which supplies eight electrons as is the case with eight Li per

cell.²² If we can dope more electrons into β - B_{105} , the donated electrons will fill the IAL and trapping levels, and E_F will reach the conduction band; thus metal transition and superconductivity can be expected.

In this study, we report Mg doping of higher concentration into β - B_{105} without Si doping. We also discuss the structure and electronic properties of Mg-doped β - B_{105} and the possibility of metal transition and superconductivity.

II. EXPERIMENT

Mg was doped into β - B_{105} by vapor diffusion process (VDP), which is essentially the same method used in previous studies of Li or Mg doping into β - B_{105} .^{19,22} β - B_{105} powder (2N or 5N purity) and Mg granules (3N purity) were placed at both ends of a boron nitride (BN) crucible, and a BN spacer was placed to separate B and Mg. The crucible was sealed in an evacuated quartz tube and heated at 973–1473 K for 1–100 h. To measure the electrical conductivity, some samples were sintered by spark plasma sintering (SPS) at 1273 K for 10 min.

The samples were investigated by x-ray diffraction (XRD) with $CuK\alpha$ radiation in the 2θ range from 10° to 80° . The lattice constants were determined by calibrating the angle using Si powder mixed with the samples as an internal standard substance. The XRD patterns were analyzed by the Rietveld method using the program RIETAN-2000.³¹ The magnetic susceptibility was measured using a superconducting quantum interference device (SQUID) magnetometer at 1 T from 2 to 300 K, and under conditions of zero-field cooling (ZFC) and field cooling (FC) at 10 Oe from 2 to 100 K to examine superconductivity. The magnetization curve was also measured from -2 to 2 T at 37.5, 100, 200, and 300 K. The electrical conductivity was measured from 50 to 300 K using the van der Pauw method.

III. RESULTS AND DISCUSSION

A. Structure

For the Rietveld refinement, we selected doping sites of the Mg and Si atoms in accordance with the literature. We assumed the doping sites for Si to be the A_1 and $B1$ sites,^{1,17} and for Mg to be the D , E , and F sites^{22,32} and the recently suggested the new site.^{33,34} We named this new site the H site, although Giunchi *et al.* named it the N site.³⁴ We measured only one sample (Mg- β -9) using synchrotron radiation powder diffraction.³⁵ The result of Rietveld refinement shown in Table II is almost consistent with the result of conventional XRD. We checked the possibility of Mg occupation at the B_{12} center or at the A_1 , A_2 , A_3 , F_1 , or G site;³⁶ however, the occupancies of these sites were found to be zero. Because it is difficult to determine site occupancies of the minor B sites, from $B(B16)$ to $B(B20)$, by conventional XRD measurement, they were fixed to be 0. Table II shows the VDP or SPS conditions, the composition of the unit cell, the lattice constants of the hexagonal unit cell, the occupancies of the partially occupied sites (D , E , F , H , $B4$, and $B13$ sites), and the reliability factors R_{wp} and S , which are the results of the Rietveld refinement of undoped and Mg-doped

TABLE II. Vapor diffusion processing (VDP) or spark plasma sintering (SPS) conditions, compositions of unit cell, lattice constants of hexagonal unit cell, occupancies of partially occupied sites and reliability factors, and R_{wp} and S obtained by Rietveld refinement of undoped and Mg-doped β -B₁₀₅, respectively. The samples were arranged according to Mg content. The analysis was performed without considering B(B16) to B(B20). β -B₁₀₅ is only the ideal structural formula and differs from the actual composition B_{106.6}. Mg- β -N-SPS indicates that the sample was prepared by SPS from Mg- β -N. The results of our synchrotron radiation powder diffraction (SR) (Ref. 35) and those of Mg-doped β -B₁₀₅ analyzed by other groups are also shown (Ref. 32–34).

Sample name	VDP/SPS condition	Composition	Lattice constant (Å)		Occupancy (%)						R_{wp}	S
			a_{hex}	c_{hex}	Mg(D)	Mg(E)	Mg(F)	Mg(H)	B(B4)	B(B13)		
β -B ₁₀₅ (2N)		B ₁₀₄	10.932(1)	23.823(2)	0	0	0	0	100	75(1)	15.5	3.6
Mg- β -1	1473 K, 10 h	Mg _{2.8} Si _{0.4} B ₁₀₃	10.966(1)	24.066(4)	30.6(7)	51(1)	0	0	100	72(3)	15.4	3.4
Mg- β -2	1473 K, 10 h	Mg _{3.1} Si _{0.7} B ₁₀₁	10.977(1)	24.017(2)	29.1(4)	47.7(6)	5.9(1)	0	86(1)	65(1)	11.2	2.2
Mg- β -3	1273 K, 10 h	Mg _{4.7} B ₁₀₁	10.987(3)	24.138(5)	43.5(6)	91(1)	5(1)	0	92(2)	56(2)	12.2	1.7
Mg- β -4	1073 K, 100 h	Mg _{4.9} B ₁₀₁	10.985(1)	24.140(2)	46.9(4)	91.7(6)	4.9(9)	0	85(1)	66(1)	9.62	1.6
Mg- β -5	1273 K, 1 h	Mg _{5.3} B ₁₀₁	10.968(1)	24.122(2)	51.5(4)	93.3(7)	5.5(8)	0	91(1)	54(1)	10.6	2.2
Mg- β -6	1073 K, 10 h	Mg _{5.3} B ₁₀₀	10.991(1)	24.145(3)	47.7(5)	84.4(8)	11(1)	1.5(5)	76(2)	57(1)	11.9	2.1
Mg- β -7 (5N)	1073 K, 100 h	Mg _{5.5} B ₁₀₂	11.008(3)	24.240(8)	45.0(8)	95(1)	13(1)	2.0(9)	85(2)	73(4)	13.4	4.9
Mg- β -8	1073 K, 10 h	Mg _{5.7} B ₁₀₀	10.982(1)	24.132(2)	50.0(4)	99.8(7)	10.9(7)	0	86(1)	50(2)	11.1	2.4
Mg- β -9 (5N)	1073 K, 100 h	Mg _{6.1} B ₁₀₂	11.009(2)	24.236(4)	46.5(9)	100	16(1)	5(1)	88(2)	82(4)	12.1	3.6
Mg- β -10	973 K, 100 h	Mg _{6.2} B ₉₉	10.988(1)	24.121(2)	54.9(6)	98.6(9)	15.7(9)	0	78(2)	50(2)	8.75	1.8
Mg- β -11	1273 K, 1 h	Mg _{6.4} B ₁₀₁	10.996(1)	24.153(3)	56.9(5)	94.8(8)	14.2(9)	4.2(4)	85(2)	62(2)	8.91	1.5
Mg- β -12	1273 K, 10 h	Mg _{6.7} B ₉₉	11.002(1)	24.157(2)	55.1(5)	88.1(8)	21.4(8)	5.1(5)	68(1)	58(2)	10.1	3.6
Mg- β -13	973 K, 10 h	Mg _{6.8} B ₁₀₂	11.016(2)	24.175(6)	54.2(9)	86(1)	10(1)	20.6(7)	87(2)	75(3)	13.8	2.6
Mg- β -14	1073 K, 10 h	Mg _{7.3} B ₁₀₁	11.015(1)	24.167(1)	59.3(6)	91.8(9)	22.4(9)	10.1(5)	84(2)	64(2)	12.7	4.5
Mg- β -15	1073 K, 10 h	Mg _{7.3} B ₁₀₀	11.017(2)	24.181(3)	60.7(5)	89.6(8)	21(1)	9.9(5)	78(2)	61(2)	7.2	1.5
Mg- β -16	1073 K, 1 h	Mg _{7.6} B ₁₀₁	11.026(1)	24.190(3)	57.1(5)	84.1(7)	17(1)	24.1(5)	85(2)	69(2)	10.0	2.2
Mg- β -17	1073 K, 10 h	Mg _{7.9} B ₉₉	11.024(1)	24.178(2)	62.0(5)	86.0(8)	23.8(7)	17.2(5)	71(2)	61(2)	10.4	3.0
Mg- β -17 (SR)	1073 K, 10 h	Mg _{7.8} B ₁₀₁	11.0236	24.189	60.2	86.1	21.6	19.7	83.0	69.8	2.9	
Mg- β -18	973 K, 10 h	Mg _{8.4} B ₁₀₀	11.029(1)	24.184(2)	61.0(7)	79.9(9)	20.6(9)	31.9(6)	74(2)	68(2)	11.2	3.9
Mg- β -19	1073 K, 1 h	Mg _{8.5} B ₁₀₁	11.025(2)	24.178(4)	60.2(7)	86(1)	25(1)	27.7(8)	82(2)	62(3)	11.7	2.9
Mg- β -20	1073 K, 10 h	Mg _{8.6} B ₉₉	11.036(1)	24.219(2)	63.1(6)	80.3(9)	28.0(9)	25.6(4)	67(2)	68(2)	7.8	1.7
Mg- β -21-SPS	1273 K, 10 min	Mg _{6.9} B ₉₈	11.023(1)	24.193(2)	56.7(5)	86.4(9)	23.8(8)	6.0(5)	65(1)	60(2)	9.9	3.7
Mg- β -12-SPS	1273 K, 10 min	Mg _{7.0} B ₁₀₀	11.019(1)	24.190(2)	62.7(4)	94.7(7)	21.5(7)	0.9(4)	75(1)	60(1)	9.7	3.5
Mg- β -17-SPS	1273 K, 10 min	Mg _{7.5} B ₉₉	11.018(1)	24.182(2)	63.9(4)	88.4(6)	24.2(7)	7.7(4)	71(1)	65(2)	9.7	3.4
Mg- β -14-SPS	1273 K, 10 min	Mg _{7.7} B ₁₀₀	11.024(1)	24.180(2)	57.8(6)	82.7(9)	22.3(9)	20.6(5)	74(2)	61(2)	12.5	4.9
Mg- β -18-SPS	1273 K, 10 min	Mg _{8.1} B ₁₀₀	11.024(3)	24.190(8)	63.9(5)	87.4(7)	24.3(8)	17.2(5)	74(1)	64(2)	9.8	3.4
Brutti <i>et al.</i>		Mg _{5.2} B ₁₀₂	10.9830(4)	24.156(2)	49	88	8	0	92	59		
Adasch <i>et al.</i>		Mg _{5.9} B ₁₀₂	10.992(2)	24.161(4)	53.3(2)	91(1)	7.2(12)	6.7(7)	92(2)	64(2)		
Giunchi <i>et al.</i>		Mg _{8.0} B ₁₀₀	11.0402(3)	24.198(1)	50	50	16.7	50	83.3	50	12.8	

β -B₁₀₅, respectively. We use the sample names listed in Table II to denote a sample in the order of Mg content. Mg was successfully doped in large amounts into β -B₁₀₅ without Si doping, up to MgB_{11.5} (8.6 Mg per cell), by annealing at less than 1273 K. It was found that vapor Mg reduced the quartz tube to atomic Si above 1473 K and Si was doped into β -B₁₀₅. It is considered that we achieved electron doping over the IAL and trapping levels of up to approximately 17 electrons per cell because the trapping levels are much sparser than the IAL.²³

Hereinafter, we discuss the structure of the samples doped with only Mg. Figures 2(a) and 2(b) show the correlations

between the number of doped Mg and the lattice constants. The results were fitted by a linear least-squares method using

$$a = 1.1 \times 10^{-2} x_{Mg} + a_0, \quad (1a)$$

$$c = 4.9 \times 10^{-2} x_{Mg} + c_0, \quad (1b)$$

where a and c are the lattice constants of the samples, a_0 and c_0 are the lattice constants of the raw material, and x_{Mg} is the number of doped Mg/cell. The obtained gradients are similar to those of the codoping of Mg and Si, namely, 1.1×10^{-2} and 7.4×10^{-2} Å/cell, respectively.²² Figures 3(a)–3(c) show

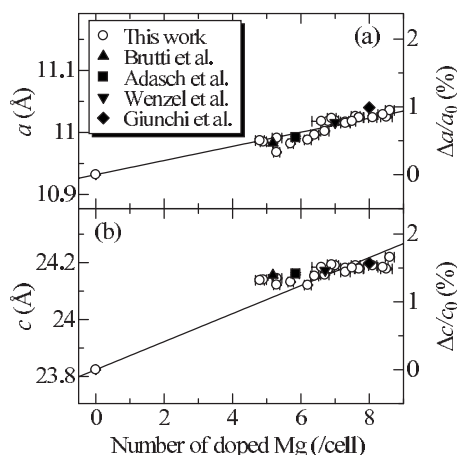


FIG. 2. Correlation between number of doped Mg and lattice constants of Mg-doped β -B₁₀₅ in the (a) a -axis and (b) c -axis directions. The results of other Mg-doped β -B₁₀₅ are also shown (Refs. 32–34 and 38). The solid lines indicate fitted Eqs. (1a) and (1b). The number of doped Mg per cell of Wenzel *et al.* was calculated using these equations.

the relationships between the number of doped electrons and the occupancies of all partially occupied sites, Mg(D), Mg(E), Mg(F), Mg(H), B($B4$), and B($B13$). It is confirmed that Mg(F) is doped with substituting B($B4$).^{32,33} The occupancy of Mg(E) decreased with Mg doping in large amounts. This is because Mg moved from the E site to the H site whose multiplicity is three times higher than that of the E site to accept more Mg. On the other hand, in spite of their close distance, no relationship is observed between the occupancy of Mg(D) and that of B($B13$), which is the defect site of β -B₁₀₅.

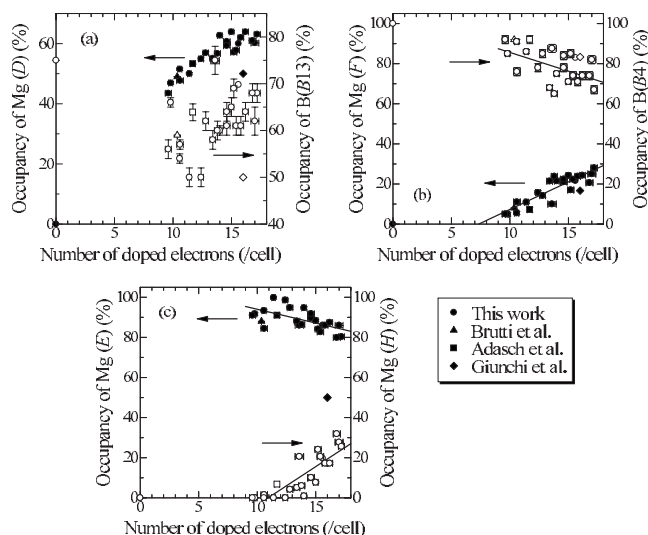


FIG. 3. Relationships between number of doped electrons and (a) occupancies of Mg(D) and B($B13$), (b) those of Mg(F) and B($B4$), and (c) those of Mg(E) and Mg(H). The filled and open symbols are for the left and right axes, respectively. The solid lines indicate the least-squares fit of the data. The results of other Mg-doped β -B₁₀₅ are also shown (Refs. 32–34).

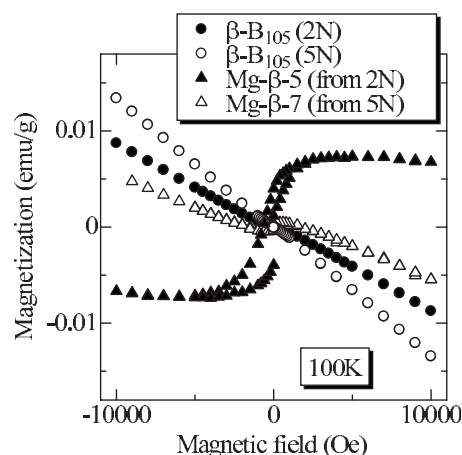


FIG. 4. Magnetization curves of undoped and Mg-doped β -B₁₀₅ prepared from 2N and 5N materials.

From this result, it seems that the solubility limit of Mg in β -B₁₀₅ is approximately eight Mg per cell (approximately MgB₁₂). The observation of MgB₁₂ (Refs. 37 and 38) and MgB_{12.5} (Ref. 39) as impurities in MgB₂ production, which are no doubt to be Mg-doped β -B₁₀₅, also indicates it. The occupancies of Mg(D) and Mg(F) were at most approximately 66% and 33%, respectively, i.e., Mg occupied 4/6 and 2/6 of the D and F sites, respectively, whereas Mg completely occupied the E site. Up to now, there is no report on a metallic element that occupies the D and F sites more than Mg, except Li which completely occupies the D site.³ The reason for the partial occupation of the F site may be that the additional defects of B($B4$) does not allow β -B₁₀₅ to preserve its structure. On the other hand, the reason for the partial occupation of the D site is not a structural problem as in the case of the F site because the D site is completely occupied in the case of Li,³ which has almost the same ionic radius as Mg. The difference in the occupancy of the D site of Li and Mg may originate from the difference in the charge of the cation of them, as Adasch *et al.* pointed out.³³

B. Magnetic susceptibility

Although we measured the magnetic susceptibility of Mg-doped β -B₁₀₅ from 2 to 100 K under conditions of ZFC and field cooled, no indication of superconductivity was observed. Figure 4 shows the magnetization curves of undoped and Mg-doped β -B₁₀₅. More prominent ferromagnetism was observed for Mg-doped β -B₁₀₅ prepared from 2N materials than for undoped β -B₁₀₅ and Mg-doped β -B₁₀₅ prepared from 5N materials. Although ferromagnetism arose from Mg doping, it was hardly observed in the samples prepared from 5N materials. Therefore, it is considered that ferromagnetism originates from impurities affected some kind by Mg doping in 2N β -B₁₀₅. We measured the magnetization curve at 37.5, 100, 200, 300, and 350 K. As a result, it was found that the saturation magnetization M_s has a linear temperature dependence, as shown in Fig. 5. Although we cannot definitely identify the material, it was thought that the ferromagnetic impurity causing ferromagnetism was derived from a Fe³⁺

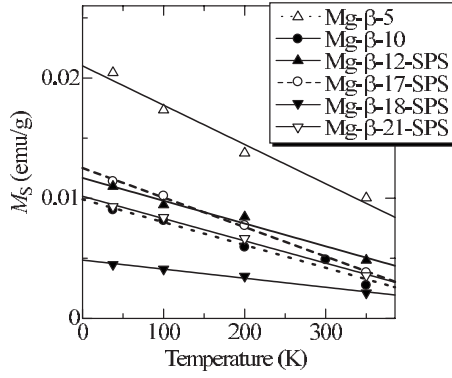


FIG. 5. Temperature dependence of saturation magnetization M_S of Mg-doped β -B₁₀₅ prepared from 2N materials. The solid, dashed, and dotted lines indicate fitted $M_S = AT + B = \chi_F(T) \times H$.

system material (FeBO₃ and/or MgFeBO₄).^{40,41}

Figure 6 shows the temperature dependence of the magnetic susceptibility χ of undoped and Mg-doped β -B₁₀₅. χ was analyzed using

$$\chi = \chi_0 + \chi_{CW} + \chi_F(T) = \chi_0 + \frac{C}{T - \theta_p} + \frac{AT + B}{H}, \quad (2)$$

where χ_0 is a temperature-independent term. The second term χ_{CW} is a term that obeys the Curie-Weiss law, where C is the Curie constant and θ_p is the Weiss temperature. The third term $\chi_F(T)$ is a ferromagnetism term represented by M_S/H , because the measurements were performed under a magnetic field that was stronger than the saturation magnetic field. As described above, because M_S/H depends linearly on temperature in this temperature range, as shown in Fig. 5, we assumed that $M_S = AT + B = \chi_F(T) \times H$, where A and B are proportionality constants. The data in Fig. 6 were fitted using Eq. (2), and χ_0 , C , and θ_p were obtained as fitting parameters. The results are shown in Table III with the values of M_S , A , and B . Figure 7 shows the relationship between C and the number of doped electrons. Our previous results of Li doping and the codoping of Mg and Si into β -B₁₀₅ are also

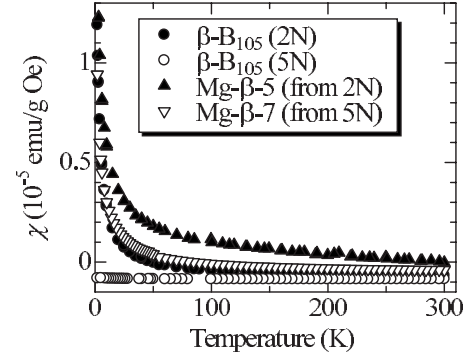


FIG. 6. Temperature dependence of magnetic susceptibility χ of undoped and Mg-doped β -B₁₀₅ prepared from 2N and 5N materials.

shown.^{19,22} To determine the number of doped electrons per atom, it was assumed that Li and Mg donate one and two electrons, respectively, and Si replacing a B atom donates one electron. C is given as $C = N\mu_B^2 p_{\text{eff}}^2 / 3k_B$, where N is the spin density, μ_B is the Bohr magneton, p_{eff} is the effective Bohr magneton, and k_B is the Boltzmann constant. We calculated N assuming $p_{\text{eff}} = 1$; as a result, N is very small and less than 1% of B and/or doped Mg contributes to χ_{CW} . Thus, it is considered that the observed χ_{CW} originates from the impurity. C reached its maximum value when the number of doped electrons was approximately 8 and vanished when the number of doped electrons exceeded 16; however, the reason for and significance of this change are not yet clear.

$\Delta\chi_0$, which is the change in χ_0 due to the doping, is given as

$$\Delta\chi_0 = \Delta\chi_p + \Delta\chi_L = \mu_B^2 \Delta N(E_F) \left\{ 1 - \frac{1}{3} \left(\frac{m}{m^*} \right)^2 \right\}, \quad (3)$$

where χ_p is the Pauli paramagnetism, χ_L is the Landau diamagnetism, $\Delta N(E_F)$ is the difference in $N(E_F)$ caused by the doping, and m^* is the effective mass; we assumed that $m^* = m$. The $\Delta N(E_F)$ values obtained from this equation are shown in Table III. Figure 8(a) shows the relationship be-

TABLE III. Temperature-independent magnetic susceptibility χ_0 , Currie constant C , Weiss temperature θ_p , saturation magnetization M_S at 100 K, proportionality constants of $M_S = AT + B$, and difference in $N(E_F)$ caused by Mg doping.

Sample name	Composition	χ_0 (10^{-7} emu/g Oe)	C (10^{-5} emu K/g Oe)	θ_p (K)	M_S (100 K) (10^{-3} emu/g)	A (10^{-5} emu/g K)	B (10^{-2} emu/g)	$\Delta N(E_F)$ (states/eV cell)
β -B (2N)	B ₁₀₄	-8.8	4.2	-1.3	0.58			0.0
Mg- β -5	Mg _{5.3} B ₁₀₁	-5.1	6.7	-2.6	8.2	-1.9	0.99	22
Mg- β -10	Mg _{6.2} B ₉₉	-4.1	3.8	-1.4	17	-3.3	2.1	28
Mg- β -21-SPS	Mg _{6.9} B ₉₈	-6.1	2.7	-1.4	8.4	-1.9	1.0	16
Mg- β -12-SPS	Mg _{7.0} B ₁₀₀	-6.3	3.9	-1.5	4.1	-0.75	0.49	15
Mg- β -17-SPS	Mg _{7.5} B ₉₉	-3.6	3.2	-1.2	10	-2.5	1.3	32
Mg- β -18-SPS	Mg _{8.1} B ₁₀₀	-5.6	0.96	-0.74	9.5	-1.9	1.2	19
β -B (5N)	B ₁₀₄	-8.9	0.087	-12	0.34			0.0
Mg- β -7 (5N)	Mg _{5.5} B ₁₀₂	-6.5	4.4	-2.5	1.5			14
Mg- β -9 (5N)	Mg _{6.1} B ₁₀₂	-6.0	3.4	-2.4	1.7			18

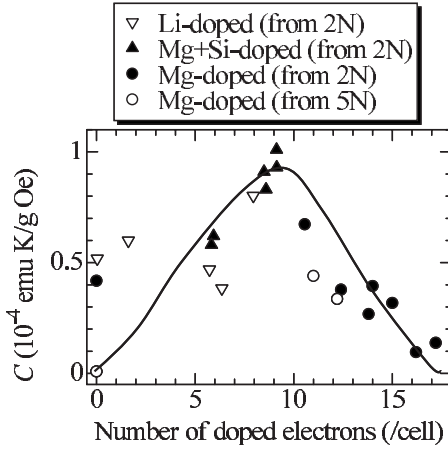


FIG. 7. Relationship between number of doped electrons and Curie constant C . Our previous results of Li doping and the codoping of Mg and Si into β -B₁₀₅ are also plotted (Refs. 19 and 22). To determine the number of doped electrons per atom, it was assumed that Li and Mg donate one and two electrons, respectively, and Si replacing a B atom donates one electron. The solid line is shown to assist viewing.

tween the number of doped electrons and $\Delta N(E_F)$. Our previous results are also shown,^{19,22} and the number of doped electrons was assumed to be the same as that in Fig. 7. This dependence of $\Delta N(E_F)$ on the number of doped electrons is discussed later with the results of the electrical conductivity in Sec. III C.

C. Electrical conductivity

Mg doping into β -B₁₀₅ bulk samples was performed; however, Mg was not doped homogeneously except in the vicinity of the surface. Thereat, Mg was doped almost homogeneously into β -B₁₀₅ powder with a particle diameter less than 45 μ m, which was then sintered by the SPS. In this way, homogeneously Mg-doped β -B₁₀₅ bulk samples were prepared. The sintered samples were crushed and analyzed

by XRD. Table II also shows the SPS conditions and the results of Rietveld refinement. Almost no difference in structure was observed after the SPS. Therefore, no defection of Mg due to sintering occurred. However, the bulk densities were about 50%, since the sintering temperature was too low.

Figure 9 shows the temperature dependence of the electrical conductivity σ of undoped and Mg-doped β -B₁₀₅. σ increased by several orders of magnitude with Mg doping, but it still showed variable-range hopping (VRH) behavior as in the case of β -B₁₀₅ and Li-doped β -B₁₀₅. Therefore, the E_F was in the localized state and even the metal transition was not observed for the sample doped with more than four Mg per cell, for which it is considered that E_F reaches the conduction band over the IAL and trapping levels. According to Mott's law for three-dimensional VRH conduction,⁴² σ is given as

$$\sigma = \sigma_0 \exp \left\{ - \left(\frac{T_0}{T} \right)^{1/4} \right\}, \quad \left(T_0 = \frac{60\alpha^3}{\pi k_B N(E_F)} \right), \quad (4)$$

where σ_0 is a constant and α^{-1} is the localization length of the wave function of the carrier. We assumed α^{-1} to be ~ 1 Å. Figure 8(b) shows the relationship between the number of doped electrons and $N(E_F)$, which was obtained from the slope of the curve in Fig. 9 using Eq. (4). We also plotted our previous results of Li doping and the codoping of Mg and Si from Refs. 19 and 22. The number of doped electrons was assumed to be the same as that in Sec. III B.

$\Delta N(E_F)$ can be approximated to be $N(E_F)$, because undoped β -B₁₀₅ is a semiconductor with $N(E_F)$ close to zero. $N(E_F)$ and $\Delta N(E_F)$, obtained from electrical conductivity and magnetic susceptibility, respectively, showed almost the same behaviors. The difference between the absolute values of $N(E_F)$ and $\Delta N(E_F)$ may originate from the hypothesis on localization length and effective mass. In the region where the number of doped electrons was less than 8 (dashed line), with increasing number of doped electrons, $N(E_F)$ increased and reached its maximum when the number of doped electrons is approximately 5 (half-filled). With supplying more

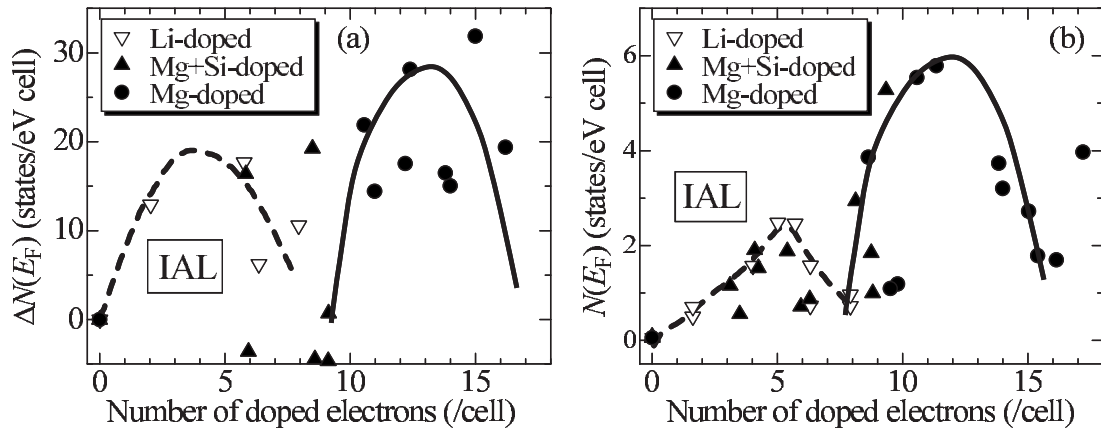


FIG. 8. Relationships between number of doped electrons and (a) $\Delta N(E_F)$ and (b) $N(E_F)$ obtained from magnetic susceptibility and electrical conductivity, respectively. Our previous results of Li doping and the codoping of Mg and Si into β -B₁₀₅ are plotted (Refs. 19 and 22). The number of doped electrons per atom was determined as in Fig. 7. The solid and dashed lines are shown to assist viewing.

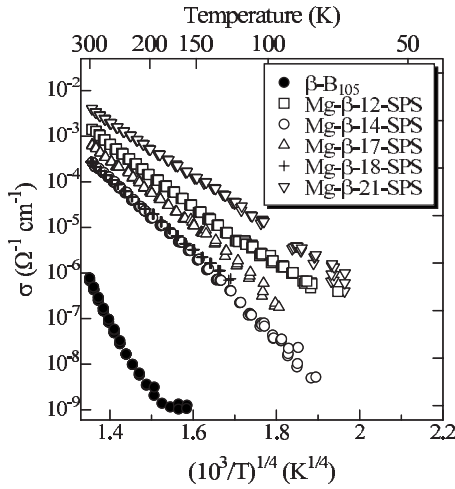


FIG. 9. Temperature dependence of electrical conductivity σ of undoped and Mg-doped β -B₁₀₅.

electrons, $N(E_F)$ turned to decrease and became almost the same value as β -B₁₀₅ when the number of doped electrons is approximately 8 (completely filled). This increasing and decreasing behavior of $N(E_F)$, which were researched in a previous study on Li doping into β -B₁₀₅,¹⁹ indicates the filling of the IAL. On the other hand, the increasing and decreasing behavior of $N(E_F)$ in the region where the number of doped electrons is more than 8 (solid line) indicates the DOS figure of β -B₁₀₅ at an energy higher than that of the IAL, which is clarified for the first time due to Mg doping. With increasing number of doped electrons, $N(E_F)$ showed the increasing and decreasing behaviors once more as in the case of doping less than eight electrons. Therefore, the existence of another localized state above the IAL was indicated. It is because E_F was in this localized state that neither metal transition nor superconductivity was observed, in spite of the electron doping over the IAL.

According to the band scheme in Ref. 23, the IAL is considered to contribute to S2, because S1 and S2 are almost occupied and unoccupied, respectively. After the electrons finished occupying the IAL, they should occupy six trapping levels from the lower energy side. If E_F is in the trapping level, the thermally activated conduction between the trapping level and the conduction band seems to be dominant, whereas the hopping-type conduction in the trapping levels is excluded. In this case, with increasing number of doped electrons, the activation energy must decrease monotonously, i.e., the slope of the curve in Fig. 9, which is proportional to the fourth root of the activation energy, must decrease monotonously. However, the slope, which is proportional to $N(E_F)$, shows the increasing and decreasing behaviors [see Fig. 8(b)]. The possibility that this newfound localized state is one of the trapping levels is also excluded because the trapping levels are much sparser than the IAL and cannot accept eight electrons as in the case of the IAL. Therefore, the contribution of trapping levels to electrical conduction should not be dominant in this system.

It is possible that this newfound localized state is the gap state originating from the defects of B(B4) caused by Mg doping, which belongs to the B₂₈ cluster. In Fig. 3(b), Mg starts to occupy the F site when the number of doped electrons is approximately 8, i.e., B(B4) starts to defect after the IAL has been occupied. It seems that the localized state arises in order for Fermi energy not to reach the conduction band and to keep the energy of the system lower. The complete occupation of this newfound localized state in spite of the parallel increase of the capacity of it and the number of doped electrons from Mg(F), which are proportional to the amount of the defects of B(B4) in this hypothesis, may originate from the occupation of Mg(H), which can donate three times electrons than Mg(E) and accelerate the occupation of this newfound localized state. Mg starts to occupy the H site when the number of doped electrons was approximately 12 where $N(E_F)$ turned to decrease. However, this possibility is too difficult to discuss in detail at present and research to test this possibility is now in progress,³⁵ because it has been shown that Mg doping influences the structural defects that originally exist in β -B₁₀₅,^{33,35} which are the origin of the IAL according to Refs. 28–30. It was found that it is difficult for β -B₁₀₅ to achieve metal transition and superconductivity because of the localized states originating from the electron deficiency and structural defects in the B₂₈ cluster.

IV. CONCLUSION

A large amount of Mg was successfully doped into β -B₁₀₅, up to MgB_{11.5} (8.6 Mg per cell), by improving VDP conditions. The electron doping at more than eight electrons/cell was achieved, i.e., E_F reached the upper state above the IAL. Nevertheless, E_F was in the localized state, and neither metal transition nor superconductivity was observed. This newfound localized state probably originates from the defects of B(B4) caused by Mg doping, which belongs to the B₂₈ cluster. It was found that it is difficult for β -B₁₀₅ to achieve metal transition and superconductivity because of the localized states originating from the electron deficiency and structural defects in the B₂₈ cluster, which is unique to β -B₁₀₅. Taking this result into account, we should aim at high- T_C superconductivity using not β -B₁₀₅, but other B-ICS without B₂₈ cluster that includes structural defects, such as α -B₁₂ or α -tetragonal B.^{43,44}

ACKNOWLEDGMENTS

The authors thank Nakamura (Department of Materials Science, The University of Tokyo) for the Electron Probe Microanalysis and I. Oguro (Institute for Solid State Physics, The University of Tokyo) for support in the magnetic measurements using SQUID. This research was supported by the Mitsubishi Foundation and Grants-in-Aid for Scientific Research from Japan Society for the Promotion of Science (JSPS) and the Ministry of Education, Culture, Sports, Science and Technology of Japan (MEXT).

*hyodo@phys.mm.t.u-tokyo.ac.jp

[†]Present address: Victor Company of Japan, Limited, 12, Moriyacho 3, Kannagawa-ku, Yokohama 221-8528, Japan.

- ¹M. Vlasse and J. C. Viala, *J. Solid State Chem.* **37**, 181 (1981).
- ²H. K. Clark and J. L. Hoard, *J. Am. Chem. Soc.* **65**, 2115 (1943).
- ³M. Kobayashi, I. Higashi, H. Matsuda, and K. Kimura, *J. Alloys Compd.* **221**, 120 (1995).
- ⁴A. F. Hebard, M. J. Rosseinsky, R. C. Haddon, D. W. Murphy, S. H. Glarum, T. T. M. Palstra, A. P. Ramirez, and A. R. Kortan, *Nature (London)* **350**, 600 (1991).
- ⁵O. Gunnarsson, *Rev. Mod. Phys.* **69**, 575 (1997).
- ⁶S. Gunji and H. Kamimura, *Phys. Rev. B* **54**, 13665 (1996).
- ⁷Y. Koike, S. Tanuma, H. Suematsu, and K. Higuchi, *J. Phys. Chem.* **41**, 1111 (1980).
- ⁸A. Oshiyama, S. Saito, N. Hamada, and Y. Miyamoto, *J. Phys. Chem. Solids* **53**, 1457 (1992).
- ⁹S. Mizuno, H. Hiramoto, and K. Nakao, *J. Phys. Soc. Jpn.* **56**, 4466 (1987).
- ¹⁰U. Mizutani, T. Kondow, and T. B. Massalski, *Phys. Rev. B* **17**, 3165 (1978).
- ¹¹J. Nagamatsu, N. Nakagawa, T. Muranaka, Y. Zenitani, and J. Akimitsu, *Nature (London)* **410**, 63 (2001).
- ¹²K.-P. Bohnen, R. Heid, and B. Renker, *Phys. Rev. Lett.* **86**, 5771 (2001).
- ¹³J. Kortus, I. I. Mazin, K. D. Belashchenko, V. P. Antropov, and L. L. Boyer, *Phys. Rev. Lett.* **86**, 4656 (2001).
- ¹⁴N. Vast, S. Baroni, G. Zerah, J. M. Besson, A. Polian, M. Grimsditch, and J. C. Chervin, *Phys. Rev. Lett.* **78**, 693 (1997).
- ¹⁵M. Calandra, N. Vast, and F. Mauri, *Phys. Rev. B* **69**, 224505 (2004).
- ¹⁶C. Wood and D. Emin, *Phys. Rev. B* **29**, 4582 (1984).
- ¹⁷G. A. Slack, C. I. Hejna, M. F. Garbaskas, and J. S. Kasper, *J. Solid State Chem.* **76**, 52 (1988).
- ¹⁸G. Will and B. Kiefer, *Z. Anorg. Allg. Chem.* **627**, 2100 (2001).
- ¹⁹H. Matsuda, T. Nakayama, K. Kimura, Y. Murakami, H. Suematsu, M. Kobayashi, and I. Higashi, *Phys. Rev. B* **52**, 6102 (1995).
- ²⁰H. Matsuda, N. Tanaka, T. Nakayama, K. Kimura, Y. Murakami, H. Suematsu, M. Kobayashi, and I. Higashi, *J. Phys. Chem. Solids* **57**, 1167 (1996).
- ²¹T. Nakayama, J. Shimizu, and K. Kimura, *J. Solid State Chem.* **154**, 13 (2000).
- ²²K. Soga, A. Oguri, S. Araake, M. Terauchi, A. Fujiwara, and K. Kimura, *J. Solid State Chem.* **177**, 498 (2004).
- ²³R. Schmechel and H. Werheit, *J. Solid State Chem.* **154**, 68 (2000).
- ²⁴H. Werheit and R. Schmechel, in *Semiconductors: Non-Tetrahedrally Bonded Elements and Binary Compounds I*, Landolt-Börnstein, Group III, Vol. 41, Part C, edited by O. Madelung (Springer, Berlin, 1998), pp. 3–148.
- ²⁵H. Werheit, M. Laux, and U. Kuhlmann, *Phys. Status Solidi B* **176**, 415 (1993).
- ²⁶R. Franz and H. Werheit, *Europhys. Lett.* **9**, 145 (1989).
- ²⁷M. Fujimori and K. Kimura, *J. Solid State Chem.* **133**, 178 (1997).
- ²⁸R. Schmechel and H. Werheit, *J. Phys.: Condens. Matter* **11**, 6803 (1999).
- ²⁹Y. Imai, M. Mukaida, M. Ueda, and A. Watanabe, *J. Alloys Compd.* **347**, 244 (2002).
- ³⁰D. L. V. K. Prasad, M. M. Balakrishnarajan, and E. D. Jemmis, *Phys. Rev. B* **72**, 195102 (2005).
- ³¹F. Izumi and T. Ikeda, *Mater. Sci. Forum* **321**, 198 (2000).
- ³²S. Brutti, M. Colapietro, G. Balducci, L. Barba, P. Manfrinetti, and A. Palenzona, *Intermetallics* **10**, 811 (2002).
- ³³V. Adasch, K.-U. Hessb, T. Ludwigc, N. Vojteerc, and H. Hillbrecht, *J. Solid State Chem.* **179**, 2900 (2006).
- ³⁴G. Giunchi, L. Malpezzi, and N. Masciocchi, *Solid State Sci.* **8**, 1202 (2006).
- ³⁵S. Hosoi, H. Hyodo, A. Nezu, H. Kim, K. Kirihara, K. Soga, K. Kimura, K. Kato, and M. Takata (unpublished).
- ³⁶H. Werheit, H. Haupt, T. Lundström, and I. Higashi, *Z. Naturforsch., A: Phys. Sci.* **45**, 1016 (1990).
- ³⁷R. Schmitt, J. Glaser, T. Wenzel, K. G. Nickel, and H.-J. Meyer, *Physica C* **436**, 38 (2006).
- ³⁸T. Wenzel, K. G. Nickel, J. Glaser, H.-J. Meyer, D. Eyidi, and O. Eibl, *Phys. Status Solidi A* **198**, 374 (2003).
- ³⁹G. Giunchi, C. Orecchia, L. Malpezzi, and N. Masciocchi, *Physica C* **433**, 182 (2006).
- ⁴⁰C. J. Kriessman and A. P. Greifer, in *Magnetic and Other Properties of Oxides and Related Compounds*, Landolt-Börnstein, Group III, Vol. 4, Part B, edited by K.-H. Hellwege and A. M. Hellwege (Springer, Berlin, 1970), p. 216.
- ⁴¹E. Burzo, in *Magnetic Properties of Non-Metallic Inorganic Compounds Based on Transition Elements: Boron Containing Oxides*, Landolt-Börnstein, Group III, Vol. 27, Part H, edited by H. P. J. Wijn (Springer, Berlin, 1970), p. 13.
- ⁴²N. F. Mott and E. A. Davis, *Electronic Processes in Non-Crystalline Materials*, 2nd ed. (Clarendon, Oxford, 1979).
- ⁴³Z. Wang, Y. Shimizu, T. Sasaki, K. Kawaguchi, K. Kimura, and N. Koshizaki, *Chem. Phys. Lett.* **368**, 663 (2003).
- ⁴⁴K. Kirihara, H. Hyodo, H. Fujihisa, Z. Wang, K. Kawaguchi, Y. Shimizu, T. Sasaki, N. Koshizaki, K. Soga, and K. Kimura, *J. Solid State Chem.* **179**, 2799 (2006).